



STUDYING THE EFFECT OF SURFACTANT ON VOLUME PHASE TRANSITION OF POLY N-ISOPROPYL ACRYLAMIDE MICROGELS



*Thesis Submitted in Partial fulfillment for the Award
of the Degree of
Master of Science*

By

ZOHEB ABAI

(413PH2079)

UNDER THE SUPERVISION OF

Dr. SIDHARTHA JENA

DEPARTMENT OF PHYSICS AND ASTRONOMY

2014-2015

NATIONAL INSTITUTE OF TECHNOLOGY ROURKELA

ROURKELA- 769008

ODISHA

DECLARATION

I hereby declare that the work carried out in this thesis is entirely original. It was carried out in Polymer Physics and Soft matter Laboratory in Department of Physics & Astronomy, National Institute of Technology, Rourkela. I further declare that, it has not formed the basis for the award of any degree, diploma, or similar title under any other university or institution.

Date: 12/05/2015

Zoheb Abai
Zoheb Abai

413PH2079

M.Sc. (II years)

Department of Physics & Astronomy

National Institute of Technology

Rourkela-769008



Department of Physics & Astronomy
National Institute of Technology, Rourkela
Rourkela- 769008
Odisha, India

CERTIFICATE

This is to certify that the thesis entitled, "*Studying the Effect of Surfactant on Volume Phase Transition of Poly N-isopropyl Acrylamide Microgels*" submitted by Zoheb Abai in partial fulfilment of the requirements for the award of Master of Science in Physics at National Institute of Technology, Rourkela is a bonafide work carried out by him under my supervision. To the best of my knowledge, the experimental matter embodied in the thesis has not been submitted to any other University/Institute for the award of any degree or diploma.

A handwritten signature in black ink, appearing to be 'S. Jena', with a stylized flourish at the end.

Date: 12-05-2015

Prof. Sidhartha Jena
Supervisor
Department of Physics & Astronomy
National Institute of Technology
Rourkela -769008, Odisha, India

ACKNOWLEDGEMENT

I would like to express my deep sense of gratitude to my thesis supervisor, Dr. Sidhartha Jena, Associate Professor in Department of Physics & Astronomy at National Institute of Technology, Rourkela for his valuable instructions, guidance and illuminating criticism throughout my project. Without his involvement and supervision, it would not have been possible for me to complete the project and bring it to the present conclusion.

I would like to express my sincere thanks to Miss Mithra K, Research Scholar in Department of Physics & Astronomy at National Institute of Technology Rourkela for her sincere cooperation and help throughout my project. I am also greatly thankful to Miss Santripati Khandai, Research scholar in Department of Physics & Astronomy at National Institute of Technology Rourkela for valuable guidance.

At last I would like to sincerely thank all those who have directly or indirectly helped me for the work reported here in.

ABSTRACT

We have studied the effect of anionic surfactant Sodium Dodecyl Sulfate (SDS) on volume phase transition of Poly N-isopropyl Acrylamide (PNIPAM) Microgels. Three samples were prepared with different SDS concentration and studied with the help of Dynamic Light Scattering and UV-Vis Spectroscopy. A sharp volume-phase transition was observed for all the three samples as a function of temperature. A sharp decrease in microgel particle size was observed at 34 °C for SDS concentration of 1.05 mM. Decrease in particle size both in collapsed and swollen state is observed with increase in SDS concentration. With naked eyes the samples appears more turbid at room temperature for lesser SDS concentration, which has been confirmed with the help of UV-Vis measurements.

CONTENTS

Chapter 1: INTRODUCTION

1.1 GELS AND ITS CLASSIFICATIONS

1.2 COMPARISON BETWEEN MICROGELS AND MACROGELS

1.3 POLY N-ISOPROPYL ACRYLAMIDE MICROGELS

1.4 REASONS BEHIND STUDYING PNIPAM MICROGELS

1.5 APPLICATIONS OF PNIPAM MICROGELS

Chapter 2: LITERATURE SURVEY

2.1 LCST AND RELATED THERMODYNAMICS

2.2 TYPES OF POLYMERIZATION

2.3 METHOD OF PREPARATION OF PNIPAM

2.4 LITERATURE SURVEY FOR MICROGEL SYNTHESIS

Chapter 3: SAMPLE PREPARATION

3.1 DESCRIPTION OF THE CHEMICALS FOR THE MICROGEL PREPARATION

3.2 DESCRIPTION OF PREPARATION OF PNIPAM MICROGEL SAMPLES

Chapter 4: EXPERIMENTAL TECHNIQUES

4.1 DYNAMIC LIGHT SCATTERING

4.2 UV-VIS SPECTROSCOPY

Chapter 5: EXPERIMENTAL RESULTS

5.1 DYNAMIC LIGHT SCATTERING

5.2 UV-VIS SPECTROSCOPY

Chapter 6: CONCLUSIONS

REFERENCES

CHAPTER – I

INTRODUCTION

1.1 Gels and its Classifications:

Gels are dispersion of molecules of a liquid within a solid in which solid is the continuous phase and liquid is the discontinuous phase. By weight, they are liquid, yet they behave as solids due to a 3-dimensional cross linked network within the liquid. Here cross-link can be defined as a small region in a macromolecule from which at least four chains emanate (primarily covalent bonds), but it can also be used to describe sites of weaker chemical interactions, portions of crystallites, physical interactions and entanglements. The main purpose of adding cross link agents while polymerization is to loosen the ability of polymer chains to move as an individual, thus creating a network.

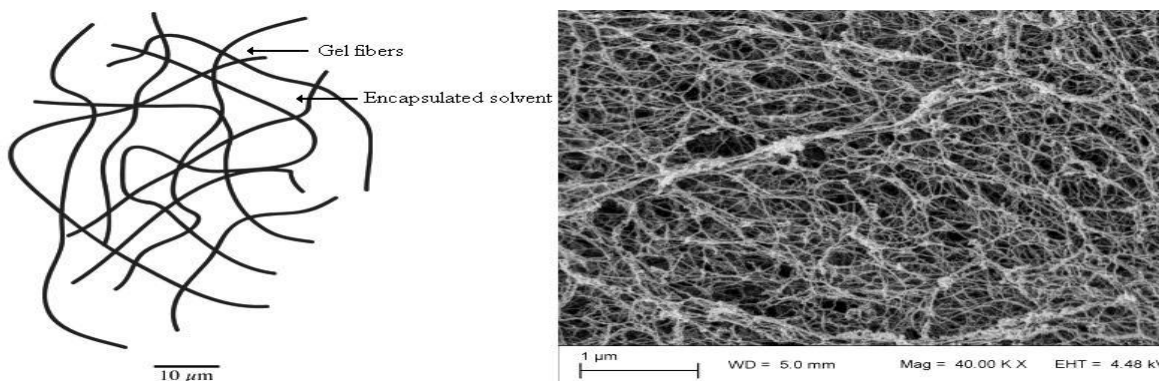


Figure 1.1: Structural Diagram of Gels

Gels are classified based upon its: (i) source, (ii) internal structure, and (iii) size

On the basis of its source: Based on its source from which it is obtained it can be classified as either natural or artificial gels. Natural gels are found in nature and some of the common examples of them are: aloe vera, jelly fish, sea algae etc., where as artificial gels are synthesized in laboratories or industries and some of the common examples are: hair gels, cosmetic products, jelly, etc.

On the basis of internal structure: Based on cross-linking types, the gels can be categorized as either physical gels or chemical gels. The cross-linking in physical gels are formed due to weak bonds like: hydrogen bond, van-der-waals forces, ionic interactions or simply by entanglement. These gels are sometimes called as weak gels. The common of examples of these types of gels are: gelatin, agarose, etc. In contrast to this chemical gels are formed due to strong forces like covalent bond resulting from chemically cross-linked bonds. Due to this, these types of gels are called strong gels. The common of examples of these gels are: Polyacrylamide gels, Poly vinyl alcohol gels, etc.

On the basis of its size: The gels may be classified based on its size as macro, micro or nano gels. Macro gels generally spans the whole space, where as micro gels are typically ranges from sub-micron to few microns in diameter. As oppose to this nano gels are typically 1 nm to few tens of nanometers.

Here, the gel under our study is Poly N-isopropyl Acrylamide (PNIPAM) microgel. PNIPAM can also be synthesized as macrogel, though it doesn't have as many applications as the microgel. So in the next section we would like to show the reasons behind the choice of microgel over macrogel.

1.2 Comparison Between Micro and Macro Gels:

Microgels are defined as colloidal dispersion of gel particles. They form an intermediate between the branched and macroscopically cross linked systems. Because of their sponge like structure they show swelling nature in suitable solvents. This swelling is dependent on degree of cross linking, polymer-solvent compatibility/interaction parameter and the presence of electrical charges. Like any colloidal dispersion, microgel particles can aggregate (flocculate or coagulate).

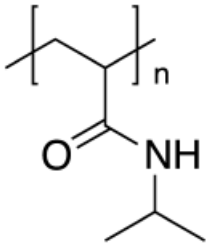
Macro and microgels have similar polymeric chemical properties, but their physical molecular arrangements differ from each other. Microgels share a number of properties with macrogels but the colloidal nature of microgels gives them significant advantages over macrogels. Some of the advantages of microgels are listed below:

- Microgel suspensions are free-flowing liquids unless highly concentrated. Their fluid properties depend upon the volume fraction of swollen particles and are approximately independent of cross-link density, whereas macrogels show fluid properties only at very low levels of cross-linking concentration and that too at near the gel point only.
- Microgels respond very rapidly to environmental changes. The very high surface to volume ratio, facilitate mass transport to and from the microgels easily.
- Exotic microgel morphologies can be used to fine-tune its properties. There is no macrogel equivalent of the wide range of core-shell particle architectures.
- Microgels can be assembled into useful larger objects such as 2D assemblies at the air-water and oil-water interfaces. Examples of 3D structures are colloidal crystals giving environmentally sensitive optical properties and layer-by-layer assemblies.

1.3 Poly N-isopropyl Acrylamide Microgels:

Over the past few decades Poly N-isopropylacrylamide (PNIPAM) has been one of the most studied temperature responsive polymer microgel having a Lower Critical Solution Temperature (LCST) of $\sim 32^\circ\text{C}$. These temperature responsive polymers are the polymers that exhibits a drastic and discontinuous change of their physical properties with temperature. They belong to a class of smart material that changes their properties in response to environmental conditions.

Some of the physical properties of PNIPAM are mentioned below:

Structural diagram	Physical properties
	<ul style="list-style-type: none"> ➤ Molecular Formula : $(\text{C}_6\text{H}_{11}\text{NO})_n$ ➤ Molar Mass: 113.16 gm ➤ Appearance: White solid ➤ Density: 1.1g/cm^3 ➤ Melting Point: 369K

1.4 Reasons Behind Studying PNIPAM Microgels:

Poly N-isopropyl acrylamide microgels when heated in water above 32 °C, undergoes a reversible lower critical solution temperature (LCST) phase transition from a swollen hydrated state to a shrunken dehydrated state, losing about 90% of its volume. PNIPAM contains hydrophobic as well as hydrophilic moiety. The isopropyl moiety is hydrophobic whereas the amide moiety is hydrophilic. Water behaves as a good solvent through hydrogen bonding with amide groups at room temperature. This hydrogen bonding with water gets increasingly disrupted on heating causing water to act as a poor solvent leading to a gradual chain collapse. Inter- and Intra-polymer hydrogen bonding and polymer-polymer hydrophobic interactions becomes dominant above the LCST. Thus it changes its nature from hydrophilicity to hydrophobicity and vice-versa abruptly at its LCST. This thermally induced de-swelling nature (inverse solubility upon heating) of PNIPAM is the main area of our study.

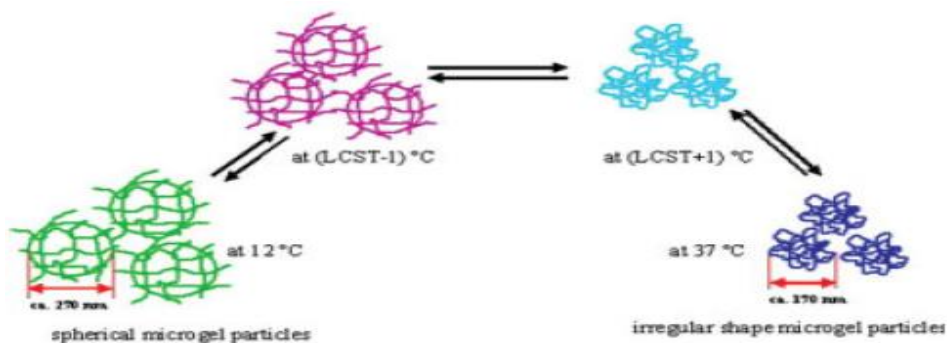


Figure 1.2: Volume phase transition of PNIPAM microgels

1.5 Applications Of PNIPAM Microgels:

The biggest driving force for PNIPAM microgel research is that it can be intelligent or responsive, meaning their degree of swelling can be tuned by temperature, pH, magnetic fields, light, and specific solutes such as glucose. Controllable swelling has been applied to demonstrate the uptake and release of solutes, including drugs, proteins, and surfactants. Thus areas concerning profound applications of PNIPAM microgels are:

Drug delivery systems: PNIPAM based gels can be conjugated with specific molecules for site specific drug delivery, therefore reducing the side effects and increasing the therapeutic activity of drugs. The drugs to be delivered are incorporated within the microgels and delivered to the

target site. At the target site, they are exposed to a temperature above LCST as a result of which the polymer collapses and releases the drug.

Separation Media: The peculiar characteristic of PNIPAM has been utilized for the regulation of cell attachment and detachment on/from matrices which are grafted with PNIPAM-based polymers by the change in temperature. Above the LCST, the PNIPAM microgels are hydrophobic and interact with the components of the cells while below that they are hydrophilic and do not interact with them.

Photo-dynamic Therapy: PNIPAM based hydrogels can be utilized for photodynamic therapy and drug delivery driven photo-thermally. In such cases, photosensitive moieties are attached to PNIPAM hydrogels and volume phase transitions are achieved by irradiating the entire system at resonance wavelength of photosensitive moieties. Upon irradiation, the light energy is absorbed and gets converted into heat energy. As a result, the hydrogels get heated up and the temperature rises beyond LCST of the polymer which results in its deswelling. If the drug is loaded within the microgel, shrinking of the same leads to the release of drug at target site.

Bio-Sensors: PNIPAM hydrogels can be utilized in biosensing as it can provide a three dimensional environment for biological interactions. The hydrogels provide inert surfaces that prevent non-specific adsorption of proteins. Biological molecules can be easily bonded to the hydrogels and thus change their property in response to external environmental conditions like temperature, pH, ionic concentration etc.

Thus, PNIPAM promises to be a smart polymer for its applications especially in drug delivery systems. However, being non-biodegradable, questions of its toxicity still arise and hence considerable research is being carried out on its safety aspects.

CHAPTER 2

LITERATURE SURVEY

2.1 LCST and Related Thermodynamics:

Lower Critical Solution Temperature (LCST) is the critical temperature below which the components of a mixture are miscible for all compositions. The word 'lower' indicates that the LCST is a lower bound to a temperature interval of partial miscibility or miscibility for certain components only. Here miscibility means the property of substances to mix in all proportions. Partially miscible polymer solutions often exhibit two solubility boundaries, the Upper Critical Solution Temperature (UCST) and LCST, where both of them depend on degree of polymerization, polydispersity, branching, polymer's composition and its architecture.

The prime physical factor here is that LCST phase separation is driven by unfavorable entropy of mixing. Since mixing of the two phases is spontaneous below the LCST and not above, the Gibbs energy change ΔG for the mixing of these two phases is negative below the LCST and positive above, and the entropy change $\Delta S = \frac{d(\Delta G)}{dT}$ is negative for this mixing process. It should be noted here that this is in contrast to more common and intuitive cases in which entropies drive mixing due to increased volume accessible to each component upon mixing. This unfavorable entropy of mixing responsible for the LCST has either of the following physical origins:

- ❖ Associating interactions between the two components such as polar interactions or hydrogen bonds, which prevents random mixing. Thus below LCST mixing occurs not due to entropy but due to enthalpy of formation of hydrogen bonds.
- ❖ Compressibility effects in polymer-solvent system. Mixing process requires contraction of the solvent for the compatibility of the polymer, resulting in a loss of entropy.

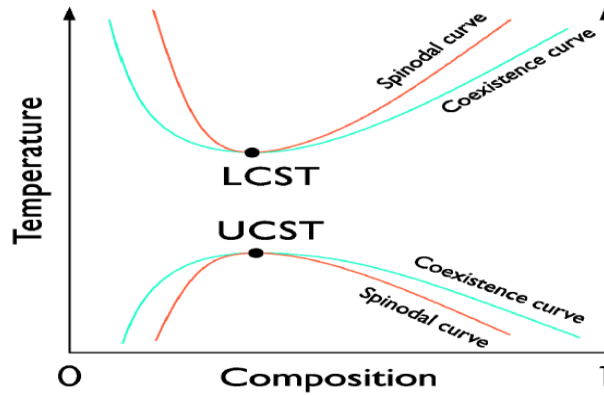


Figure 2.1: Plot of typical polymer binary solution phase behavior

With the help of statistical mechanics, the Gibbs free energy change for mixing of a polymer with a solvent can be derived from Flory-Huggins Solution Theory. Although the theory makes simplifying assumptions, it generates useful results for interpreting experiments. Thus for constant external pressure and temperature, Gibbs free energy change is given as:

$$\Delta G = \Delta H - T\Delta S$$

And the result obtained by Flory and Huggins is:

$$\Delta G = RT[n_1 \ln \phi_1 + n_2 \ln \phi_2 + n_1 \phi_2 X_{12}]$$

where, n_1 = Number of moles of solvent, ϕ_1 = volume fraction of solvent, n_2 = number of moles of polymer, ϕ_2 = volume fraction of polymer, X_{12} = Interdispersing energy of polymer and solvent molecules, R is the gas constant, and T is the absolute temperature.

For small solute, the mole fractions would appear instead of volume fractions. For PNIPAM microgel LCST happens to be around 32 °C.

2.2 Types Of Polymerization:

There are generally four types of polymerization process for the preparation of microgel particles:

1. **Emulsion Polymerization (EP):** This is a very versatile technique which yields narrow particle size distributions. It can be performed in the presence of added surfactant, known as Conventional Emulsion Polymerization, or in the absence of added surfactant, known

as Surfactant Free Added Polymerization (SFEP). In SFEP, the continuous phase have a high dielectric constant (e.g. water) and ionic initiators are employed (e.g. potassium persulfate). Due to difficulty of completely removing residual surfactant in Conventional EP method, SFEP is widely used for the preparation of PNIPAM, as it does not suffer from this residual surfactant contamination problem.

2. **Anionic Copolymerization:** This method usually produces mono-disperse particle distributions since micelle particle distributions of block copolymers dispersed in solvent are usually narrow. The particle size reported here indicates considerable aggregation of block copolymer within micelles prior to cross linking. Here the initial micelle size determines the final microgel particle size.
3. **Inverse micro-emulsion Polymerization:** Here the monomers consists both anionic and cationic parts. The copolymerization is initiated using UV irradiation and the product formed is isolated and re-dispersed in aqueous electrolyte solutions. The particles get swelled in the presence of high electrolyte concentration as a result of screening of the attractive electrostatic interactions between neighboring chains.

2.3 Method of Preparation of PNIPAM:

PNIPAM microgels are synthesized mainly by EP method. The PNIPAM monomer and cross linking agent methylene-bis-acrylamide (BIS) are mixed in water under a nitrogen atmosphere. Different amount of Sodium Dodecyl Sulphate (SDS) in water are used as a surfactant to control the particle size. Pottasium persulfate (KPS)-water solution is added to the reactor to initiate the polymerization. The reaction is kept at 70°C for 4 hours. After cooling the solution to room temperature, the final reaction dispersion is exhaustively dialyzed in a dialysis tube to wash out unreacted chemicals and surfactant.

The figure below shows salient features of EP:

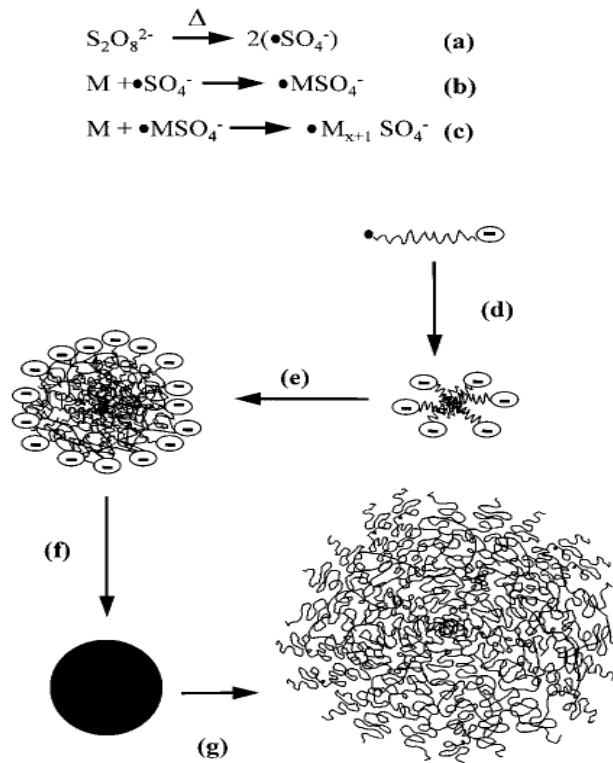


Figure 2.2: Mechanism for the preparation of microgel particles by EP. The steps shown are initiator decomposition (a) initiation, (b) propagation, (c) particle nucleation, (d) particle aggregation, (e) particle growth in a poor solvent, (f) and particle swelling in a good solvent, (g). The counter-cations and the particle charges for steps (f) and (g) have been omitted for clarity. M represents a vinyl monomer.

Here thermal decomposition of the ionic initiator $\text{S}_2\text{O}_8^{2-}$ initiates free-radical polymerization. The oligomers produced are surface active and form nuclei when the length of the oligomers exceeds the solubility limit of the solvent. The nuclei then undergo limited aggregation, thereby increasing the surface charge until electrostatic stabilization is achieved. Further particle growth occurs through absorption of monomer and/or oligomeric chains. This process results in a decrease in the concentration of oligomers to below the critical value required for particle formation. Polymerization continues within the particles until another radical species enters the growing particle and thus termination occurs.

With the help of observed value of mean polymer density ($M/N_A/V_h$) of microgel particles the water content in swollen state (below LCST) of PNIPAM has been observed between 88-99%, while for collapsed state (above LCST) between 40-65%.

It has also been observed that monodispersed PNIPAM particles can also be formed during SFEP in the absence of added cross linking monomers. This shows that NIPAM acts as its own cross linking monomer, however the efficiency of cross linking is clearly improved when cross linking monomers are employed.

2.4 Literature Survey for Microgel Synthesis:

Tata et al. synthesized aqueous suspensions of PNIPAM nanogel particles by free radical precipitation polymerization process. Here, 139mM of N-isopropylacrylamide, 1.96mM of N, N'-methylene-Bisacrylamide and 1.05mM of sodium dodecyl sulfate (SDS) were dissolved in 250ml of Argon purged water. Then the reaction mixture was kept at 70°C for one hour and then 2.22mM of potassium persulphate (KPS) was added with vigorous stirring. The polymerization was carried out at 70°C for 4hours under a stream of Argon.

Yang et al. synthesized PNIPAM microgel particles by free radical precipitation polymerization method. Here, 2.26g of N-isopropylacrylamide, 0.03g of N, N'-methylene-bisacrylamide and 0.03g of sodium dodecyl sulfate(SDS) was dissolved in 161 mL of water in a 250mL three-necked round-bottomed flask equipped with a condenser and a gas inlet under continuous magnetic stirring. The aqueous solution was purged with nitrogen for about 30min and then heated to 70°C. Then, 0.09g of Potassium persulfate was added to initiate polymerization. The polymerization was performed under a nitrogen atmosphere for 4.5h at 70°C.

Wu et al. synthesized PNIPAM microgel by taking 240mL dust-free deionized water, 3.84 g NIPAM, 0.0730g BIS and 0.0629 g SDS in a 500 mL reactor fitted with a glass stirring rod, a teflon paddle, a reflux condenser and a nitrogen bubbling tube; then, the solution was heated to 70°C and stirred at 200 rpm for 40 min with a nitrogen purge to remove oxygen; finally, 0.1536 g KPS dissolved in 25mL dust-free deionized water was added to start the polymerization. The reaction mixture was stirred for 4.5 h. Then the microgel particles were purified and diluted for LLS measurements.

Varga et al synthesized PNIPAM microgels following the method of Wu et al. In this method 7.0g NIPAM, varying amount of cross-linker BIS (0.000-0.700 g) and 94 mg SDS was dissolved in 470 mL distilled water. The temperature of the reactor was kept at 60°C and solution was

intensively stirred. To remove oxygen, nitrogen gas was purged through the solution for 30 min. Then, 0.14 g APS dissolved in 30 mL water was mixed with the solution and it was followed by intensive stirring for 4hrs. Eight PNIPAM samples were prepared with different crosslink densities depicted by notation (molar ratio of the NIPAM monomer to the cross-linker BIS) N13, N30, N50, N70, N200, N300, N400, polymer (without cross-linker).

Wu et al prepared four different samples of PNIPAM microgel having respective SDS concentration of 0mM, 1.42mM, 2.6mM, 9.5mM. They observed in their results that microgel particles are narrowly distributed with an initial average hydrodynamic radius of 180nm and it swells as $C_{(SDS)}$ increases. When $C_{(SDS)}$ is higher than 2.6mM, the radius of the microgel particle reaches its limit value of 250nm and the maximum relative increases in radius is ca. 40%. These results are explained by the theory that SDS molecules forms micelles inside the network. The repulsion between the micelles and the gel network extend the network. As $C_{(SDS)}$ increases, more SDS micelles are formed inside the network so that the particle swells further. However, the number of the micelles able to exist inside the microgel network is limited. When that limit is reached, the swelling ceases. Further with the help of the above explanation, here two step volume phase transition model is also approached. The first step involves the breaking up of the micelles and expelling of SDS from the gel network, while the second step represents collapse of the surfactant-free gel network.

Napper et al prepared 10 different samples of PNIPAM microgel having SDS concentration as 30mg/L, 73mg/L, 145mg/L, 291mg/L, 436mg/L, 727mg/L, 1017mg/L, 1235mg/L, 1453mg/L, 2300mg/L. They observed in their results that during gradual increase of SDS concentration from zero to CMC while microgel formation, the collapse transition became sharper and approached a cooperative first-order-like transition at the higher SDS concentrations. They explained this nature by relating it to an intricate balance between the attractive and repulsive components of several different types of forces, which includes the interactions between PNIPAM segments in the inner layer, the hydrophobic interactions between the PNIPAM chains and SDS molecules, the interactions between the PNIPAM-SDS complexes and counter-ions, as well as the interactions between the ion pairs. At lower SDS concentrations, there was no apparent interaction between the interfacial chains and surfactant molecules. The collapse transitions observed presumably resulted from the intramolecular interactions (n-clusters) of the interfacial

PNIPAM chains. As the surfactant concentration was increased, SDS was cooperatively bound to the interfacial PNIPAM chains through hydrophobic interactions which lead to stable dimensions of the interfacial PNIPAM chains. The osmotic pressure inside the interfacial PNIPAM chains is also increased due to an increase in the concentration of mobile counter-ions and so the transitions become sharper.

Snowden et al prepared 7 different samples of PNIPAM microgels having respective SDS concentration as 0mM, 2mM, 3mM, 4mM, 6mM, 9mM and 12mM. They observed in their results that by the addition of anionic surfactant SDS to microgel results in an increase in conformational transition temperature of the particles. They also observed that for SDS concentrations of 4mM and above, swelling of particle takes place under isothermal conditions.

Anderson et al prepared 4 different samples of PNIPAM microgels having respective SDS concentration as 0.4mM, 1.3mM, 4.0mM and 6.7mM. They observed in their results that by increasing the surfactant concentration in microgel results in decrease in its swelled hydrodynamic radius with its corresponding increase in VPTT. They explained their results by assigning the role of SDS in the particle nucleation to increase the colloidal stability of precursor particles and thus lowering the diameter of primary particles as the number of particles is increased.

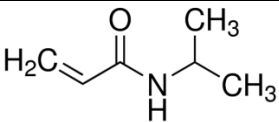
Abuin et al prepared 3 different samples of PNIPAM microgels having respective SDS concentration as 0mM, 2.5mM, 4.0mM. They observed that the binding of SDS to PNIPAM causes the average particle diameter to decrease and the temperature at which the volume phase transition occurs, shift to higher temperatures.

CHAPTER 3

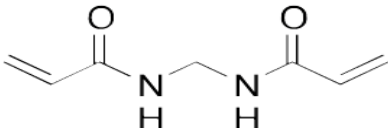
SAMPLE PREPARATION

3.1 Description of the Chemicals for the Microgel Preparation:

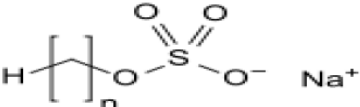
Monomer: N-isopropyl acrylamide (NIPAM). This is the monomer unit from which PINAM is synthesized by polymerization.

Structural diagram	Physical properties
	<ul style="list-style-type: none">➤ Molecular formula: C₆H₁₁NO➤ Molar mass: 113.16 gm

Cross-linker: N,N'-Methylenebisacrylamide (BIS). It's a cross-linking agent used during the formation of polymers. It polymerizes with NIPAM and creates cross-links between PNIPAM chains, thus forming a network of PNIPAM rather than unconnected linear chains of NIPAM.

Structural diagram	Physical properties
	<ul style="list-style-type: none">➤ Molecular formula: C₇H₂N₁₀O₂➤ Molar mass: 154.17 gm

Surfactant: Sodium dodecyl Sulphate (SDS). It acts as a surfactant and is useful for formation of PNIPAM during SFEP process.

Structural diagram	Physical properties
	<ul style="list-style-type: none">➤ Molecular formula: C₁₂H₂₅SO₄Na➤ Molar mass: 288.38 gm

Initiator: Potassium Persulfate (KPS). It acts as an initiator. It initiates the polymerization reaction by free radical formation.

Structural diagram	Physical properties
$2 \text{ K}^+ \quad \text{O}^- - \text{S}(=\text{O})_2 - \text{O} - \text{O} - \text{S}(=\text{O})_2 - \text{O}^-$	<p>➤ Molecular formula: $\text{K}_2\text{S}_2\text{O}_8$</p> <p>➤ Molar mass: 270.31gm</p>

3.2 Description of Preparation of PNIPAM Microgel Samples:

The chemicals N-isopropylacrylamide (NIPAM), N,N-methylenebis-acrylamide (BIS), Potassium persulfate (KPS) and Sodium dodecyl sulfate (SDS) was obtained from Sigma Aldrich and were used without further purification.

Three samples of 50 mL each were prepared for different SDS concentration of, 1.05 mM, 2.40 mM and 4.20 mM. First 0.7864 g of NIPAM, 0.0152 g of BIS and 0.01521 g of SDS (for 1.05 mM solution) was added to 49 mL of dust free Milli-Q water in a beaker containing a magnetic bead. The beaker was kept on top of a heater cum magnetic stirrer with arrangement for nitrogen purge for synthesizing the microgels in an inert atmosphere. The solution was heated up to 70°C and stirred at 300 rpm for an hour with nitrogen purge to remove the oxygen and provide an inert environment to the sample. Finally, 0.03076 g KPS dissolved in 1mL dust-free de-ionized water was added to start the polymerization. The reaction mixture was maintained at 70°C and stirred for another 3 hours for complete polymerization. For DLS measurements the whole above procedure was carried out inside the Horizontal Laminar Flow (Model # CP- HLAF) to provide a clean and dust free environment for sample preparation. For other two samples the same above procedure was followed except 0.03460 g (2.40 mM of SDS) and 0.06056 g (4.20 mM of SDS) was added instead of 0.01521 g of SDS.

For UV-Vis Characterization 3 mL of each samples at a dilution of 1:1, 1:50 and 1:100 were prepared in a test tube. These samples were taken in quartz cuvettes for UV measurements.

CHAPTER 4

EXPERIMENTAL TECHNIQUES

4.1 Dynamic Light Scattering:

Dynamic Light Scattering also referred as Photon Correlation Spectroscopy or Quasi-Elastic Light Scattering, is a non – invasive and versatile technique to determine the dynamics of large molecules like: macromolecules, polymers, bio-polymers and proteins in solutions. Light which is an electro-magnetic wave proves suitable for probing the dynamics for these large molecules as the wavelength of light is comparable to their dimensions. When a beam of light impinges on atoms and molecules, it induces dipole moment in them, which in turn oscillates with a frequency same as the frequency of the incident beam. These oscillating dipole moments give rise to secondary radiation, popularly known as “scattered radiation or scattered light”. The intensity of the scattered light depends on the polarizability of the molecules, which can be expressed as:

$$\alpha = \frac{nM}{2\pi N_A} \left(\frac{dn}{dc} \right)$$

where α = *polarizability*, M = *molecular mass*, N_A = *Avogadro's number*, dn/dc = *concentration dependence of refractive index*.

In solutions these molecules undergo Brownian motion due to constant collisions with the solvent molecules. Thus the fluctuating dipoles keep changing their positions constantly which results in fluctuations of scattered intensity with time. Because of the Brownian motion the particles undergo frequent displacements from their positions and lead to slight variation in the frequency of scattered light as compared with the incident light. This is better known as the Doppler shift in the frequency. Because a slight frequency (equivalent to energy) change is involved in DLS it is also known as the quasi – elastic light scattering. Dynamic light scattering measures these fluctuations in the scattered intensity as a function of time. The correlation of fluctuating intensity with time will provide information about the dynamics of the system from

which the information about the particle dimension can be obtained. The figure below shows the Brownian motion of a particle and how it leads to the fluctuations in the measured intensity.

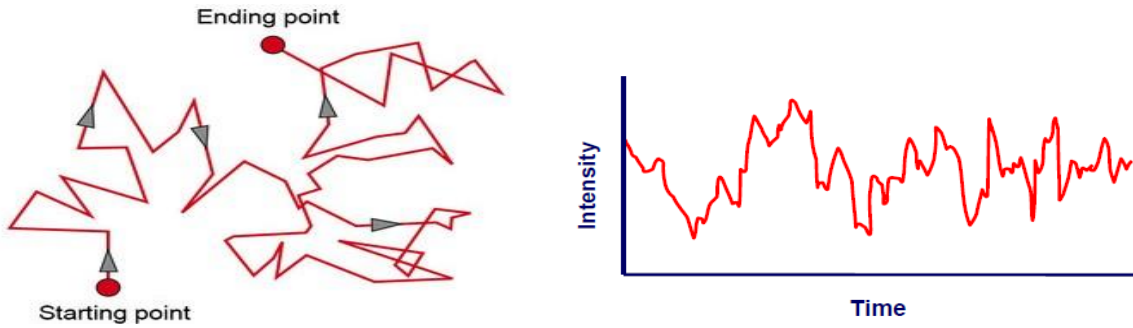


Figure 4.1: Brownian motion of molecule and resulting intensity fluctuations

The smaller particles move faster thus changing their positions more frequently as compared to larger particles, hence their intensity fluctuates more rapidly compared to the larger particles. A schematic of intensity fluctuations with time for a 4 and 40 nm particle is shown below.

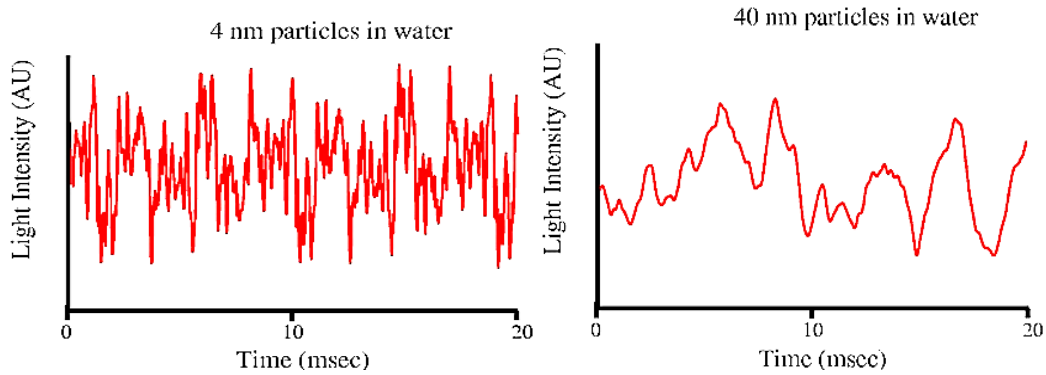


Figure 4.2: Variation of intensity according to the particle size

The particle size is one of the prime factors in deciding how well the intensity measured at time ' t ' is correlated to the intensity measured at some later time ' $t + \tau$ '. In principle the field-field correlation (ECF) contains all the information about particle dynamics in solutions. The field-field correlation function, $g_1(q, \tau)$ can be written as,

$$g_1(q, \tau) = \frac{\langle E_s(t) E_s^*(t + \tau) \rangle}{\langle |E_s(t)|^2 \rangle}$$

where $E_s(t)$ and $E_s^*(t + \tau)$ are the scattered field at time ' t ' and ' $t + \tau$ ' respectively. But experimentally one measures intensity instead of field. So in DLS one measures intensity-intensity correlation function (ICF) rather than ECF. The ICF, $g_2(q, \tau)$ can be written as,

$$g_2(q, \tau) = \frac{\langle I_s(t) I_s^*(t + \tau) \rangle}{\langle |I_s(t)|^2 \rangle}$$

where $I_s(t)$ and $I_s(t + \tau)$ are the scattered intensity at time ' t ' and ' $t + \tau$ ' respectively. The ICF and ECF are related by Siegert's relation,

$$g_2(q, \tau) = 1 + \beta |g_1(q, \tau)|^2$$

If the signal intensity at ' t ' is compared with itself then there is perfect correlation as the signals are same. If the signals at ' $t + \tau$ ', ' $t + 2\tau$ ', ' $t + 3\tau$ ', ... ' $t + n\tau$ ' are compared with the signal at ' t ', the correlation of a signal arriving from a random source will decrease with time until at some time (when ' n ' becomes large), there will be effectively no correlation between intensity at ' t ' and ' $t + n\tau$ ' no correlation. A perfect correlation is obtained at delay time of $\tau = 0$, indicated by correlation of '1' to no correlation at delay time of $n\tau = \infty$ is indicated by zero correlation of '0'.

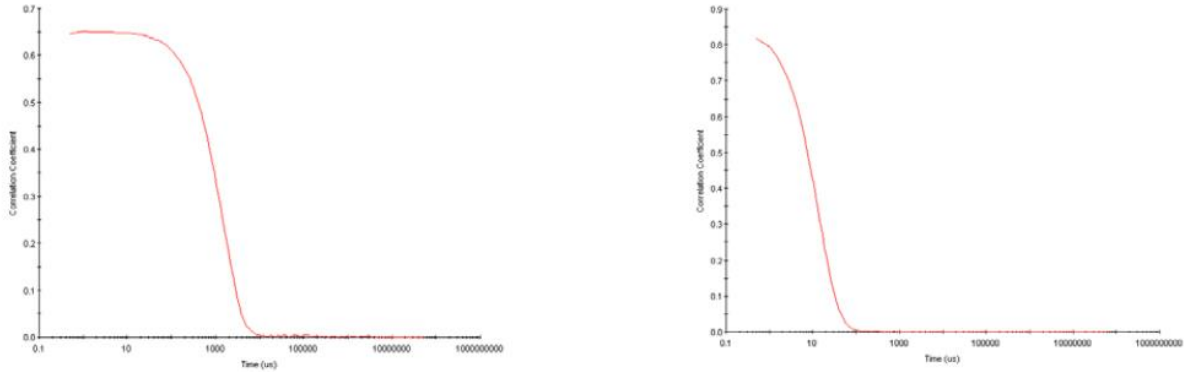


Figure 4.3: Correlator coefficient against time plot for small and large particles

If the particles are large the signal will be changing slowly and the correlation will persist for a long time. If the particles are small and moving rapidly then correlation will reduce more quickly.

The ECF is related to the decay constant (Γ) by the relation

$$g_1(q, \tau) \sim \exp(-\Gamma \tau)$$

From the decay constant, the particle's diffusion coefficient, D can be calculated by using the relation:

$$\Gamma = Dq^2$$

where, q is the scattering vector given by $q = \left(\frac{4\pi n}{\lambda}\right) \sin\left(\frac{\theta}{2}\right)$, where n = refractive index of dispersant, λ = wavelength of laser, θ = scattering angle.

Thus the size of particle is calculated from translational diffusion coefficient by using Stokes-Einstein equation given by:

$$R_h = \frac{kT}{6\pi\eta D}$$

where R_h = hydrodynamic radius, D = Translational diffusion coefficient, k = Boltzmann's Constant, T = absolute temperature, and η = viscosity

Thus in this way we get to know about the size of the particles with the help of DLS instrument. Picture of DLS and its schematic diagram is given below

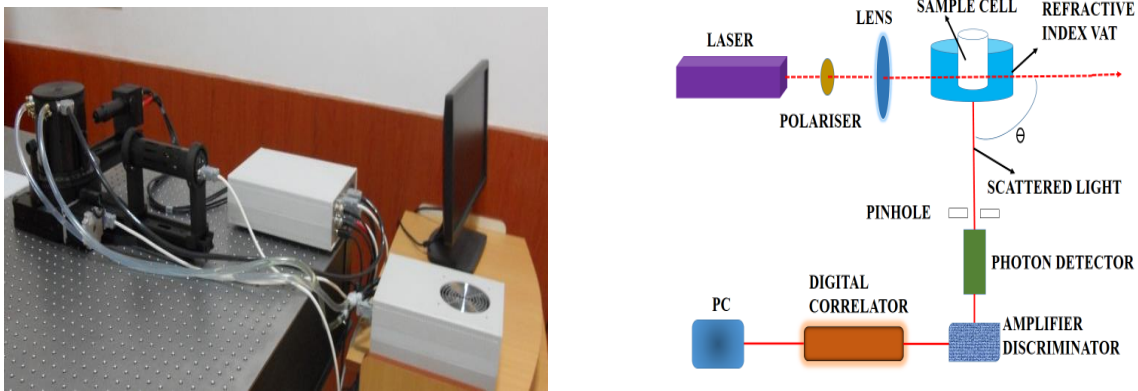


Figure 4.4: Dynamic Light Scattering setup and its and its Schematic diagram.

4.2 UV-VIS SPECTROSCOPY:

UV-Vis spectroscopy is used to measure the extent to which the samples under consideration absorbs or transmits light at different wavelengths within UV-Vis range. It measures the intensity of light, ' I ' passing through the sample against the initial light intensity ' I_0 '. The relation between these intensities is given by Beer-Lambert law:

$$I = I_0 \exp(-\mu x)$$

where, ' x ' is the path length and ' μ ' is the absorption coefficient. Now we know absorption coefficient is given as:

$$A = 2 - \log T$$

where $T = I/I_0$

And thus we can calculate turbidity τ as

$$\tau = 2.303 * (A - A_0),$$

where A_0 = Absorbance of reference

The basic parts of a UV-Vis spectrometer are a light source, a sample holder, a diffraction grating, a monochromator or a prism to separate the different wavelengths of light, and a detector. The sources of light is generally a deuterium arc lamp which provides light in ultraviolet region (190 to 350 nm) and Tungsten-Halogen lamp for visible and near infrared region (350 to 1100nm). The detector is generally a photodiode. Light passing through the cuvette containing sample falls on the mirror one (M1). The reflected light from the M1 is incident on the grating and the diffracted light from the grating is directed towards the second mirror (M2). The detector picks up the signal and displays it as a transmittance/absorbance versus wavelength spectra. From the absorbance we can calculate the value of turbidity of the sample.

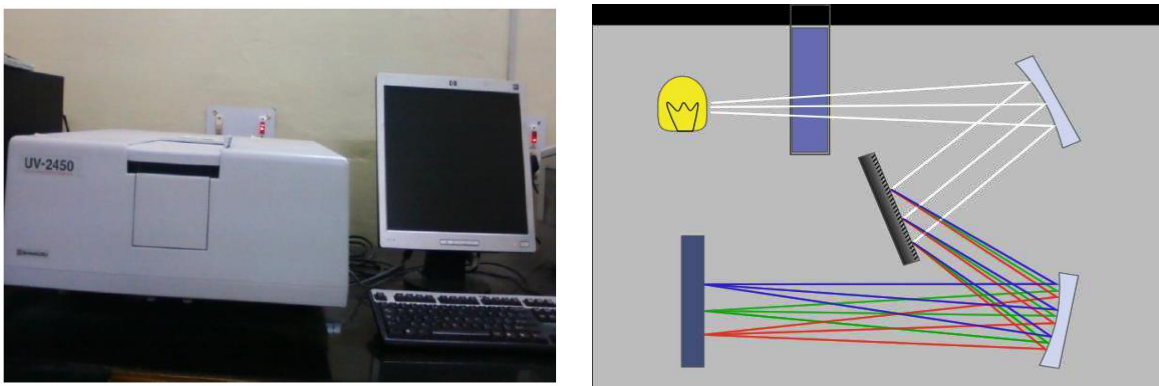


Figure 4.5: UV-Vis Spectrometer and its schematic diagram

CHAPTER 5

EXPERIMENTAL RESULTS

5.1 Dynamic Light Scattering:

The Hydrodynamic radius as obtained from dynamic light scattering measurements has been plotted against sample temperature is shown in figure below:

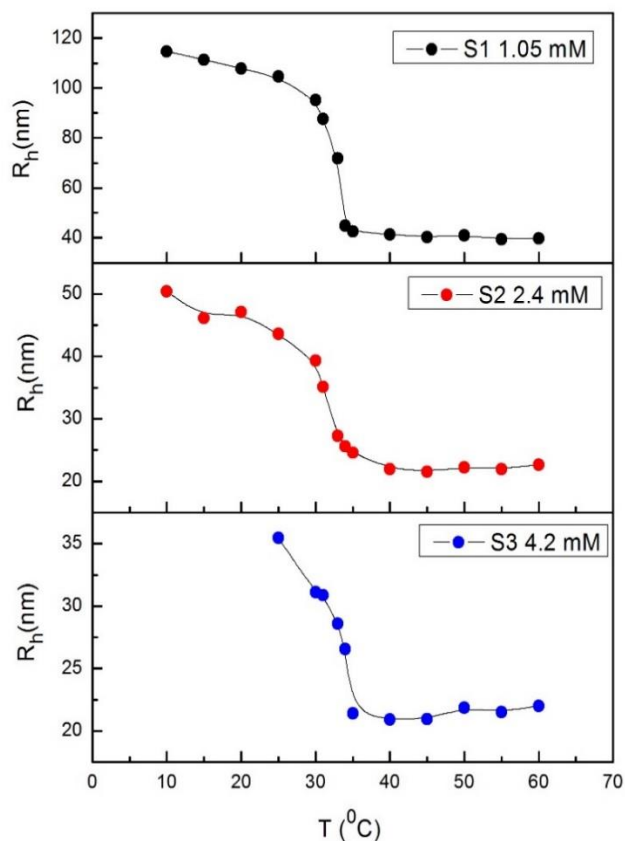


Figure 5.1: Plot of hydrodynamic radius against Temperature

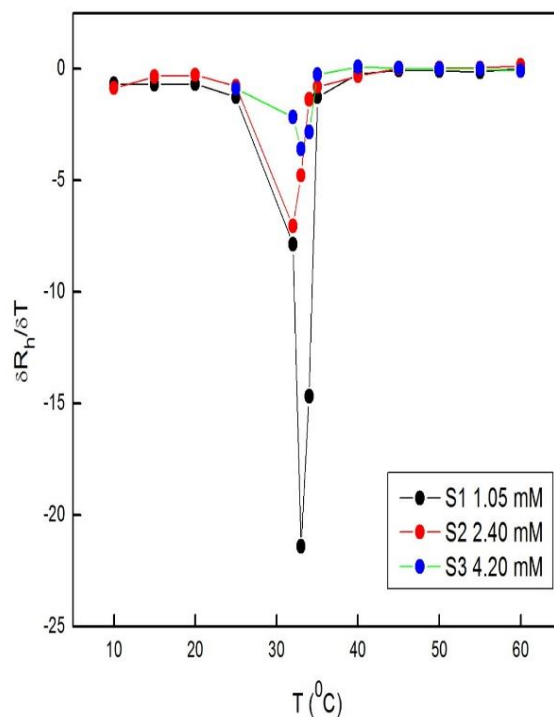


Figure 5.2: Plot of rate of change in hydrodynamic radius with respect to temperature against sample temperature

It is observed from Figure 5.1 that as the SDS concentration increases the hydrodynamic size of the particle decreases. The value of the hydrodynamic radius at 25 °C and 60 °C for all the samples is given below in Table 5.1.

Table 5.1 Table of different values of hydrodynamic radius at 25 °C and 60 °C for all three samples

Sample	SDS concentration	R_h (25°C)	R_h (60°C)
S1	1.05 mM	107.70	39.64
S2	2.40 mM	43.59	22.65
S3	4.20 mM	35.46	21.58

For all the three samples as the temperature is increased, after a certain temperature there is a sharp transition in size of the particles. Before the transition the particles are swollen, and as temperature crosses a certain temperature the particles de-swells. This transition temperature is known as Volume Phase Transition Temperature.

From the Figure 5.2 we can conclude that the volume phase transition temperature gets gradually shifted to higher temperature as SDS concentration increases. This can be explained the volume phase transition occurs by breaking up of micelles and expelling of SDS from the gel network, followed by the collapse of surfactant free gel network. So we can conclude that higher the concentration of SDS micelles inside the gel network, higher the temperature needed to expel it.

The Swollen/De-swollen ratio of microgels can be calculated by formula given as

$$\frac{\text{Volume of swollen microgel particles}}{\text{Volume of Collapsed microgel particles}} = \frac{R_s^3}{R_c^3}$$

The calculated swelling ratio for all the three samples have been plotted against temperature in the figure below

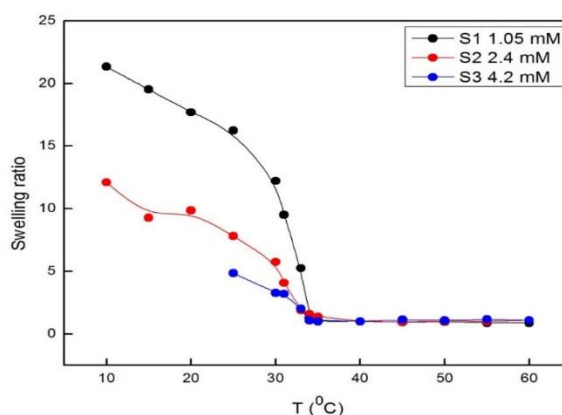


Figure 5.3: Plot of Swelling Ratio against sample Temperature

From the above graph it can be seen that the swelling ratio of all the microgel particles increased as the temperature was decreased. The PNIPAM microgels with highest SDS concentration of, 4.2 mM swelled about 5 times, while that with 2.4 mM of SDS swelled about 12 times of its original volume. For lowest SDS concentration of 1.05 mM it swelled as high as 20 times of its initial volume. The high value of swelling ratios for the larger particles can be correlated with the internal structure of the particles. Larger the diameter of the particles, more is the swelling and as the size of the particles decreases the swelling ratio also decreases.

From the above DLS results, the role of SDS in the particle nucleation can be believed to increase the colloidal stability of precursor particles and thus lower the diameter of primary particles as the number of particles gets increased. The cloud point of linear PNIPAM chains in water increases significantly with the presence of SDS. The ionic surfactant binds to the polymer above a critical association concentration, resulting in formation of a charged polymer–surfactant complex. The electrostatic repulsion between the charged complexes prevents aggregation of the polymer chains effectively above the LCST. Consequently, the polymer precipitation is affected by SDS. Thus it can logically understood that large amounts of SDS while polymerization may prevent the formation of tightly packed PNIPAM aggregates that would eventually form the permanent, solid PNIPAM particles due to crosslinking. Thus high SDS concentration shifts the polymerization system closer to the good-solvent conditions, and the microgel structure appears to be more homogenous than the samples prepared in the low surfactant concentration.

5.2 UV-Vis Spectroscopy:

Figure 5.4 shows the plot of turbidity of microgel versus wavelength for all the three samples.

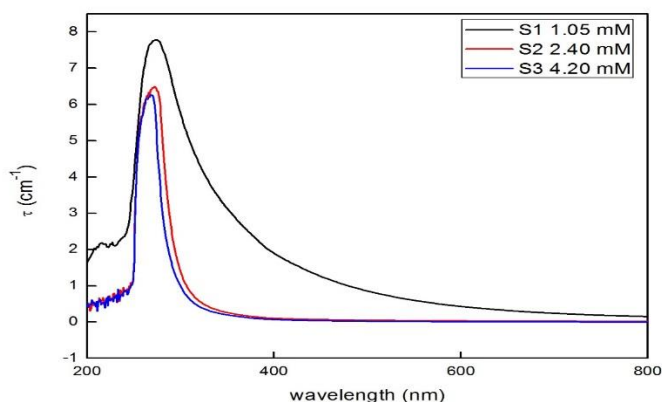


Figure 5.4: Plot of Turbidity versus wavelength for all the three samples

For PNIPAM microgel below LCST, the turbidity of the sample decreases more rapidly for greater concentration of SDS. The turbidity of the sample for higher SDS concentration (2.4 and 4.2 mM of SDS concentration) was found to negligible for wavelengths beyond 500 nm. However for sample with the lowest SDS concentration, 1.05 mM a significant amount of turbidity was observed even at higher wavelengths. Thus it can be concluded that there are minimal amount of solid (insoluble) structures at temperatures below LCST in the microgel samples with high SDS concentrations as compared to those with low SDS concentration. Thus high turbidity indicates the presence of significant fraction of permanent-solid particle structures evolved during the polymerization process. Thus it can be concluded that high SDS concentration prevents the formations of permanent, solid PNIPAM particles that would cause turbidity of the aqueous dispersions.

CHAPTER 6

CONCLUSIONS

In the present work, we studied the volume phase transition of PNIPAM microgel by varying the SDS concentration. From our study we conclude that:

- ✓ For increase in the SDS concentration, hydrodynamic radius of the particles decreases both for swollen and de-swollen states.
- ✓ The volume phase transition temperature increases for increase in SDS concentration.
- ✓ The turbidity of PNIPAM microgels decreases for increase in concentration of SDS for swollen state.

References:

1. S. Zhou, B. Chu, J. Phys. Sci. B 34 (1996) 1597.
2. S. Zhou, B. Chu, J. Phys. Chem. B 102 (1998) 1364.
3. B. Chu, Laser Light Scattering, 2nd ed., Academic Press, New York, 1991.
4. C. Wu, K. Chan, and K. Q. Xia, Macromolecules, 28 (1995)1032.
5. C. Wu and C. Y. Yan, Macromolecules, 27, 4516 (1994).
6. R. Pecora, Dynamic Light Scattering, Plenum Press, New York, 1976.
7. B. R. Saunders, B. Vincent, ACIS, 80, (1999), 1-25.
8. E. Abuin, A. Leon, E. Lissi, J.M. Varas, Colloids and Surfaces A, 147 (1999) 55–65.
9. H.G. Schild, D.A. Tirrell, Langmuir 7 (1991) 665.
10. T. Gilányi, I. Varga, R. Mészáros, G. Filipcsei and M. Zrínyi, Phys. Chem. Chem. Phys., 2, (2000) 1973.
11. B.V.R Tata and S. S Jena, Solid State Comm. 139,(2006) 562.
12. K. Kratz, T. Hellweg, W. Eimer, Polymer 42 (2001) 6631.
13. Microgel Suspensions: Fundamentals and Applications, R. Pelton and T. Hoare, ISBN: 978-3-527-32158-2, (2001).
14. I. Varga, T. Gilanyi, R. Mesza'ros, G. Filipcsei and M. Zrinyi, J. Phys. Chem. B 105 (2001), 9071
15. N. C. Woodwarda, B. Z. Chowdhrya, S. A. Leharneb, M. J. Snowden, European Polymer Journal 36 (2000) 1355
16. R. R. Kokardekar, V. K. Shah, H. R. Mody, Internet Journal of Medical Update 2012;7(2):60-63
17. H.G. Schild, Prog. Polym. Sci., Vol. 17, 163-249, 1992.
18. M. Andersson, S. L. Maunu, Journal of Polymer Science: Part B: Polymer Physics, Vol. 44, (2006) 3305–3314